

# Atherosclerotic Plaque Ultrasound Video Encoding, Wireless Transmission, and Quality Assessment Using H.264

A. Panayides, M. S. Pattichis, *Senior Member, IEEE*, Constantinos S. Pattichis, *Senior Member, IEEE*, C. P. Loizou, *Member, IEEE*, M. Pantziaris, and Andreas Pitsillides, *Senior Member, IEEE*

**Abstract**—We propose a unifying framework for efficient encoding, transmission, and quality assessment of atherosclerotic plaque ultrasound video. The approach is based on a spatially varying encoding scheme, where video-slice quantization parameters are varied as a function of diagnostic significance. Video slices are automatically set based on a segmentation algorithm. They are then encoded using a modified version of H.264/AVC flexible macroblock ordering (FMO) technique that allows variable quality slice encoding and redundant slices (RSs) for resilience over error-prone transmission channels. We evaluate our scheme on a representative collection of ten ultrasound videos of the carotid artery for packet loss rates up to 30%. Extensive simulations incorporating three FMO encoding methods, different quantization parameters, and different packet loss scenarios are investigated. Quality assessment is based on a new clinical rating system that provides independent evaluations of the different parts of the video (subjective). We also use objective video-quality assessment metrics and estimate their correlation to the clinical quality assessment of plaque type. We find that some objective quality assessment measures computed over the plaque video slices gave very good correlations to mean opinion scores (MOSs). Here, MOSs were computed using two medical experts. Experimental results show that the proposed method achieves enhanced performance in noisy environments, while at the same time achieving significant bandwidth demands reductions, providing transmission over 3G (and beyond) wireless networks.

**Index Terms**—Error resilience, flexible macroblock ordering (FMO), H.264, mobile-health (m-health), telemedicine, ultrasound video, video-quality assessment (VQA), 3G.

Manuscript received July 21, 2010; revised October 5, 2010 and December 13, 2010; accepted December 23, 2010. Date of publication January 13, 2011; date of current version May 4, 2011. This work was supported by the Research Promotion Foundation of Cyprus and the European Regional Development Fund (ERDF) under Project Real-Time Wireless Transmission of Medical Ultrasound Video ΠΙΕΝΕΚ/ΕΝΙΣΧΥ/030890.

A. Panayides, C. S. Pattichis, and A. Pitsillides are with the Department of Computer Science, University of Cyprus, 1678 Nicosia, Cyprus (e-mail: panayides@ucy.ac.cy; pattichi@ucy.ac.cy; a.pitsillides@ucy.ac.cy).

M. S. Pattichis is the director of the image and video Processing and Communications Lab, at the Department of Electrical and Computer Engineering, University of New Mexico, Albuquerque, NM 87131 USA (e-mail: pattichis@ece.unm.edu).

C. P. Loizou is with the Department of Computer Science, School of Sciences and Engineering, Intercollage, 3507 Limassol, Cyprus (e-mail: loizou.c@lim.intercollege.ac.cy).

M. Pantziaris is with The Cyprus Institute of Neurology and Genetics, 1683 Nicosia, Cyprus (e-mail: pantzari@cinc.ac.cy).

Color versions of one or more of the figures in this paper are available online at <http://ieeexplore.ieee.org>.

Digital Object Identifier 10.1109/TITB.2011.2105882

## I. INTRODUCTION

OVER the past decade, there has been an impressive growth in the development of mobile-health (m-health) systems and services [1], [2]. Technological advances in hardware, digital signal, image and video compression, and networks have significantly contributed to new m-health systems and services.

The success in the deployment of medical video streaming systems has benefited from advances in video compression technology and wireless networks infrastructure. Current state-of-the-art H.264/AVC [3] compression standard comprises efficient encoding to match the underlying transmission medium data rate, in a timely manner (real-time), and low complexity decoder. This allows for low power implementation on mobile devices. On the other hand, advances in wireless networks' infrastructure have enabled data transfer communication rates previously only available to wired infrastructures. Mobile communication networks coverage is extended between 80% and 90% of a country's region, while satellite systems practically enable communication across the globe [2].

In spite of this remarkable growth of medical video telemedicine systems, wireless channels remain error prone. Increase in available data rates is soon met by continuously increasing demands for medical video bandwidth. Different from conventional video-streaming quality requirements, the quality of medical video transmission systems is measured in terms of their diagnostic yield. The reconstruction of clinically sensitive video regions needs to be of very high quality. Degradation of clinically sensitive regions can lead to deterioration of the system's objective of remote diagnosis and care. The absence of efficient video-quality assessment (VQA) algorithms, both objective and subjective, contributes to the challenges involved in the design of a system of consistent diagnostic quality.

The motivation of this study is to develop a framework that provides: 1) a simulation environment for investigating m-health video communications over noisy wireless channels; 2) efficient ultrasound video encoding based on clinical criteria; and 3) introduce objective and subjective criteria for clinical VQA. This motivates the study of an end-to-end system that allows us to investigate how varying the encoding parameters can affect the clinical quality of the decoded video. The basic system is demonstrated on the wireless transmission of atherosclerotic plaque ultrasound videos. Here, the envisioned application scenario is to provide a system that allows clinicians to evaluate clinical ultrasound videos for emergency telemedicine applications.

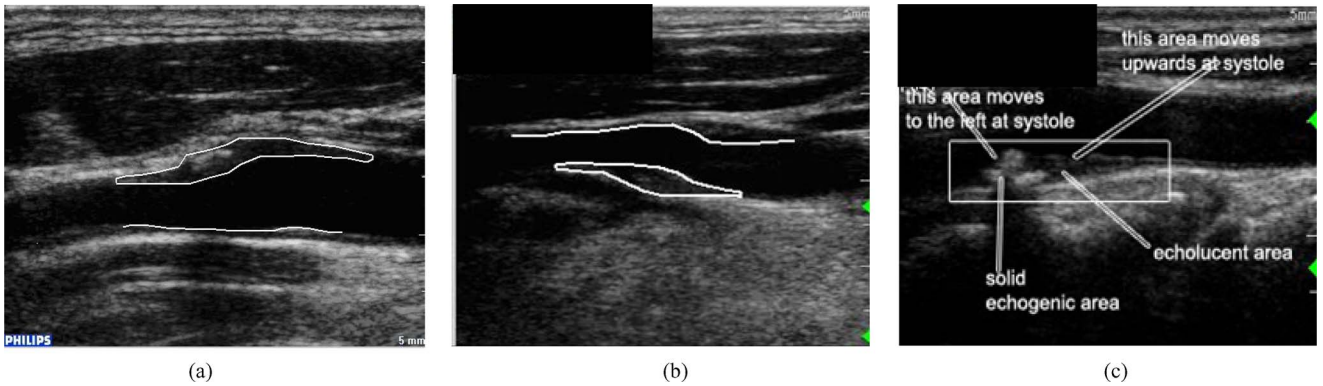


Fig. 1. Atherosclerotic plaque video image examples. The plaque boundaries and nearest walls are outlined by an automatic segmentation algorithm [22]. (a) Predominantly echogenic plaque. (b) Predominantly echolucent plaque. (c) Demonstrative plaque motion at systole and diastole with different motions for the echogenic and echolucent portions. Exam date information has been removed from (b) and (c).

TABLE I  
DIAGNOSTIC ROI CONTRIBUTION TO EACH CLINICAL RATING

|                           | Plaque<br>ROI | Wall<br>ROI | ECG | Background |
|---------------------------|---------------|-------------|-----|------------|
| Plaque boundary detection | ✓             | ✓           |     | ✓          |
| Stenosis                  | ✓             | ✓           | ✓   |            |
| Plaque Type               | ✓             |             |     |            |

Ultrasound video is widely used in vascular imaging to visualize the arterial lumen, plaque, and wall. Medical experts evaluating carotid artery ultrasound video are mainly interested in identifying plaque presence, the corresponding degree of stenosis, as well as the plaque type. Monitoring of the arterial characteristics like the vessel lumen diameter, the intima media thickness of the far wall, and the morphology of the atherosclerotic plaque are important in order to assess the severity of atherosclerosis and evaluate its progression [4].

The first objective is to ensure that the clinical data in the transmitted video is sufficient to identify the presence of the plaque and its boundary. To assess the degree of stenosis, the boundary of the plaque, its size, as well as the distance to the nearest arterial wall needs to be visualized. In Fig. 1(a) and (b), we present frames of the segmented video plaques with the associated near and far arterial walls. Furthermore, stenosis needs to be visualized throughout the cardiac cycle, over the systolic and diastolic phases, as the plaque moves [see Fig. 1(c)]. This can be facilitated by the ECG part of the video (see lower right in Fig. 3). Visualization of the echolucent and echogenic plaque regions, as well as their corresponding motions throughout the cardiac cycle is of vital importance in assessing plaque stability [see Fig. 1(c)]. The remaining part of the video carries little diagnostic information.

This paper provides a unifying framework for the following.

- 1) *Mapping clinical criteria to diagnostic encoding:* Clinical criteria are first used for determining the regions of diagnostic interest (see Table I). The regions are then used to specify video slices with independent coding control. A spatially varying quality map is used for efficient video-slice encoding.

2) *Encoding for mobile communications through noisy channels:* Wireless video transmission requires that decoding performance needs to be evaluated as a function of packet loss rates (PLRs), available bitrates, and the mobile device resolution and frame rates. A unifying framework is proposed that provides error-resilient encoding that allows for reliable performance at large PLRs.

3) *VQA based on clinical criteria:* Both objective and subjective evaluations are used for measuring the quality of the decoded video slices. To establish the validity of the approach, we use the correlation between the medical experts' mean opinion scores (MOSs) and a number of objective measurements.

4) *Coarse to fine parameter optimization based on VQA:* Here, the goal is to determine video encoding parameters that can provide acceptable video quality. The approach allows us to determine the minimum bitrates needed for transmission.

The aforementioned proposed methodology targets an encoding setting that will allow the transmission of adequate diagnostic quality video over 3G and emerging mobile telecommunications networks. Continuous medical expert feedback and objective video-quality-evaluation guide the process. Preliminary versions of this paper, using limited datasets, appear in [5]–[7].

The rest of the paper is organized as follows. Section II summarizes some related work. Section III provides the methodology. An analysis of the results is presented in Section IV. Section V provides the discussion and concluding remarks.

## II. BACKGROUND

Unique requirements associated with end-to-end medical video compression and transmission have driven a number of studies in the literature. Istepanian *et al.* [8] developed a quality of service (QoS) ultrasound streaming rate control algorithm. Based on the concept of reinforcement learning, the frame rate and quantization step are varied as a function of the state of the network. Simulations and real-time experiments validate the proposed mechanism utilizing the robotic tele-ultrasonography system OTELO [9] over 3.5G wireless networks. Results conform to a predefined medical QoS criterion. The OTELO system

is also used in [10], where multilayer control is employed to optimally tune source- and channel-encoding parameters. Frame rate, quantization step, intrarefreshing period, and average code-rate channel protection are the key parameters that are varied in these experiments.

The design of an elastic region of interest (ROI) coding that incorporates different quantization levels for ROI and non-ROI, targeting diagnostically lossless encoding over bitrate-limited wireless channels is presented in [11]. An encoder state diagram for different quality levels is designed and a state transition is considered for every group of pictures (GOP), utilizing physician expert feedback. An application in acute childhood respiratory distress is examined. A saliency-based visual attention ROI coding for low-bitrate medical video transmission is proposed in [12].

ROI coding is used for adaptive transmission of medical images in [13], as well as scalable coding of video snapshots over simulated wireless networks. Context awareness is introduced based on patient's status monitoring and resource availability of the underlying transmission medium. Scalable video coding (SVC) employing spatiotemporal scalability for a number of ultrasound videos over 3G and wireless local area networks is documented in [14]. The authors examined how wireless transmission medium parameters (data rate, packet loss, delay, jitter, and latency) relate to the diagnostic quality of the decoded video.

A synopsis of the aforementioned state-of-the-art systems reveals the current trends in the design considerations of reliable video telemedicine systems. Efficient compression methods include ROI encoding [11]–[13], SVC encoding [13], [14], while adaptive encoding taking into account underlying channel's parameters is undertaken by [8], [10], [13], and [14]. Diagnostic validation is incorporated in [8], [11], and [14].

#### *A. Objective VQA*

Objective VQA is an emerging area of active research [15], [16]. This is very different than image-quality assessment that has seen significant growth and success over the past five years.

Significant problems associated with the use of image to video-quality metrics necessitate the development of new VQA algorithms that will correlate with perceived video quality. In order to achieve this, video aspects such as motion and QoS need to be considered. Toward this direction, the National Telecommunications and Information Administration developed the video quality model (VQM) in 2004 [17]. The recently proposed motion-based video integrity evaluation (MOVIE) [16] algorithm outperforms all VQA algorithms to date [18]. Still, there is a strong demand for clinically driven video-quality metrics.

Unfortunately, our evaluation of the MOVIE and VQM algorithms showed that they do not work very well with the small sizes associated with video slices of atherosclerotic plaque ultrasound videos. In private communications with the authors of the MOVIE metric, it was suggested that this is mainly due to the relatively small sizes associated with the extracted video slices.

The peak SNR (PSNR) is still the most widely used quality metric, despite failing to efficiently assess perceived video quality [18]. The PSNR utilizes the MSE between the original and transmitted video on a frame-by-frame basis. The structure similarity index (SSIM) is another widely used metric, which was originally developed as an image-quality-assessment technique and is nowadays applied for VQA [19]. Other important methods include visual SNR (VSNR), visual information fidelity (VIF), pixel-based VIF (VIFP), information fidelity criterion (IFC), noise quality measure (NQM), and weighted SNR (WSNR). We refer to [20] for algorithmic details and implementation.

#### *B. Clinical VQA*

Clinical VQA is much more difficult than conventional objective video-quality evaluation. In fact, we often have to consider new clinical quality assessment metrics that are unique to each medical video modality. While some of the basic features of subjective quality assessment described in recommendation [21] may be employed during evaluation, clinical factors should always be considered for the proper modeling of the scoring scale.

### III. METHODOLOGY

We provide a diagram of the proposed system in Fig. 2(a)–(c). In the following, we will provide more details for each block: the process of determining diagnostic video slices, variable quality encoding, transmission, the decoded video's quality assessment, and material.

The overall system is summarized in Fig. 2(a). The clinical criteria are used to define the video encoding scheme and the VQA. For describing the channel, we provide a channel data rate and a PLR. The targeted mobile device resolution and frame rate playback is also input to the video encoding block. It is important to note that the channel may not support playback at full resolution and maximum frame rates. On the other hand, there is little reason to transmit at resolutions and frame rates that will exceed the mobile device playback abilities. This will result in unnecessary power consumption. We address these issues by determining the minimum resolutions, frame rates, and channel data rates that achieve acceptable performance.

We control the target video encoding by adjusting the quantization parameters ( $QP_1, \dots, QP_n$ ) and the rate of redundant slices (RSs). Here, the goal is to perform a coarse-to-fine parameter optimization to determine the minimum bitrates that provide diagnostically acceptable decoding. It is important to note that the term "diagnostically acceptable" is based on satisfying different clinical criteria.

The basic structure of the encoder is depicted in Fig. 2(b). Following video resolution and frame rate adjustments (see Section IV), the clinical criteria are mapped to ROIs. ROIs are mapped to video slices for independent encoding. The video quality of each slice is controlled by setting the value of the corresponding QP, with respect to its clinical significance. The video slices are then combined to reconstruct the video frames. The RS parameter is used to control error-resilient encoding. The approach here is to use a larger number of RS for recovering from larger PLRs.

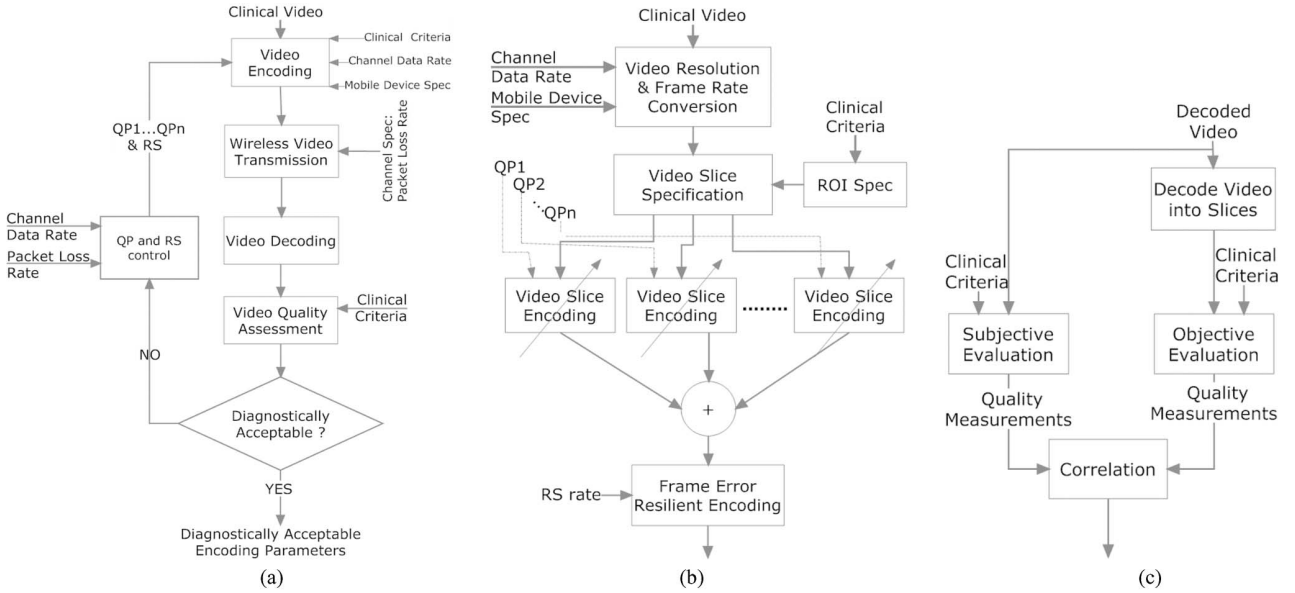


Fig. 2. (a) System diagram incorporating all steps in the design of a reliable end-to-end medical video transmission system. (b) Proposed diagnostically driven variable quality slice encoding scheme using error-resilient techniques. Channel knowledge and end-user equipment are considered during preprocessing. (c) Objective and subjective VQA and correlation.

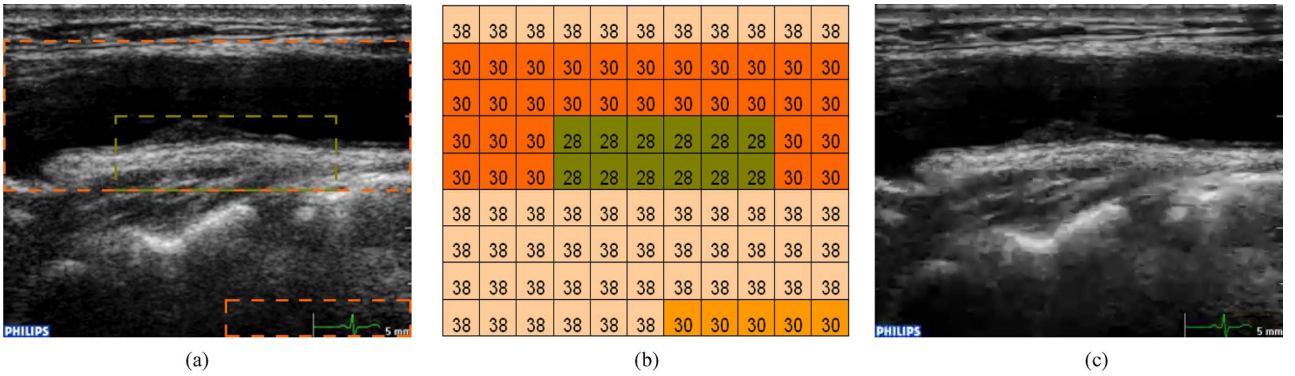


Fig. 3. Video-slice encoding and decoding. (a) Video-slice specification. (b) Corresponding QP map. (c) Decoded video using variable quality slice encoding. Here, with QPs 38/30/28 for background/wall and ECG ROIs/plaque ROI and quarter common intermediate format [QCIF-176 × 144 pixels, 11 × 9 macroblocks (MBs)].

The quality of the decoded video is assessed using both objective and subjective quality criteria [see Fig. 2(c)]. The correlation between the objective and subjective criteria is also evaluated. Ultimately, for high correlations, the objective criteria can be used to predict subjective quality. Having said this, it is often the case that high diagnostic quality can be established for high values of the objective evaluation. For example, video-slice PSNR values over a certain threshold can be used to establish that the video is of acceptable diagnostic quality. For objective video-quality criteria, we consider the video-quality metrics evaluated over the diagnostic video-slice regions (see Section II-A).

#### A. Diagnostic Video-Slice Specification

Video-slice specification requires the specification of rectangular regions over the atherosclerotic video (see Fig. 3). Here, the goal is not to provide accurate segmentation of the plaque or

the different anatomical structures of the video. Instead, we overcompensate by providing video slices that are sufficiently large to capture the plaque regions and its walls. Here, video slices are specified in terms of the boundaries of the standard (16 × 16 pixels) macroblocks (MB), which are significantly larger than the pixel-level accuracy required for video segmentation purposes.

To specify the plaque and wall video slice, we use the single-frame segmentation algorithm introduced in [22]. To account for both plaque and wall motions, we estimate the maximum motions by finding the minimum and maximum displacements over a large number of frames (considering one of every five frames for the first two cardiac cycles, and one of every ten for the remaining). This avoids the need for tracking the plaque and wall throughout the videos. For video encoding purposes, we then extend out the segmented plaque to fixed size MB boundaries [see Fig. 3(a) and (b)]. Here, note that an MB is the basic block unit that each coded frame is partitioned in all video

encoding standards since H.261 [23]. Furthermore, as noted earlier, the pixel-level accuracy of the segmentation method (given by  $0.82 \pm 0.95$  mean  $\pm$  std pixels) has a limited impact on the final video-slice specification. The wall ROI is similarly defined using the lower plaque boundary and the nearest wall. The success of this approach follows from the fact that these exams follow a clinically established protocol for visualization of the plaque type, boundary, and stenosis. The clinical protocol requires that the ultrasound probe remains steady so that the observed motion will correspond to actual plaque motion.

When the ECG video slice is to be transmitted, we simply allocate the lower right MBs for ECG [see Fig. 3(a)]. While it is not necessary here, we note that detecting the ECG is straightforward, since it is the only part of the video that appears in the green color channel.

The video-slice specification procedure can be extended to handle different scenarios by also allowing manual specification. Note that these rectangular regions can be specified quickly using two mouse clicks (for specifying any two opposing corners). Recall that the relationship between the selected video slices and the clinical criteria is given in Table I.

#### B. Variable Quality Encoding of Diagnostic Video Slices

For the purposes of this study, we need to consider the baseline profile of H.264/AVC. The baseline profile targets wireless video streaming to mobile devices, and incorporates low-complexity encoder and decoder, low power consumption, and low latency. New error-resilience features available in the baseline profile integrated in this study are flexible macroblock ordering (FMO) and RS. A thorough overview of the standard, error-resilience features, and discussion exploiting H.264/AVC in the context of IP-based networks can be found in [23]–[25]. A detailed discussion of FMO can be found in [26], [27].

We use FMO for independently encoding the diagnostic video slices. In particular, we use FMO type 2, which allows the definition of rectangular slices as foreground(s) and background. In the event of a packet containing slice data gets dropped, H.264/AVC allows the transmission of RS (an RS being a slice describing the same MBs in a bitstream).

To enable variable quality slice encoding, we modify the encoder to support a QP allocation map (QPAmap), which stores the QP of each MB [see Fig. 3(b)]. The concept is similar with MB allocation map (MBAmmap), which stores the corresponding slice number that each MB belongs to. These QP (of each video slice) are parsed via the default configuration file used by FMO type 2 to define the boundaries of the rectangular ROIs, which is accordingly modified. Employing these minor adjustments at the encoder achieves variable quality FMO slice encoding. No change is made at the decoder, and hence, the resulting bitstream is H.264/AVC compliant (recall that slices are self-contained; hence, they can be decoded independently).

Here, we use an IPPP [6] frame type encoding structure, a GOP of 15 with an I-frame inserted at the beginning of each GOP, 15 fps and a total of 100 frames per video. Simple frame copy error concealment method is applied at the decoder to reconstruct corrupted packets.

#### C. Transmission Over Wireless Channels Simulation

To simulate transmission errors resulting in packet losses, like channel fading and congestion, and also account for video degradation caused by increased latency and jitter, a modified version of the pseudorandom packet loss simulator included in JM H.264/AVC reference software [28] is used. The simulator is enhanced by adding an implementation of the random number generator described in [29] to provide significantly improved random performance. A uniform packet loss distribution was used throughout the experiments and all results were obtained by averaging ten consecutive runs. Burst errors were simulated by dropping a maximum of four consecutive packets.

JM 15.1 supports encoding but not decoding of RS; therefore, we moved this functionality to the packet loss simulator. That is, in the event of a packet drop, if the redundant representation is loss free, then that packet is kept and forwarded to the decoder. We note here that this only works, if the RS are encoded in the same quality as the original slices, an approach we adopt here.

#### D. Video-Quality Assessment

We consider independent grading of each of the three clinical diagnosis criteria listed in Table I. From Table I, we can also see how each clinical quality criterion relates to the encoding of specific ROIs. The success of the approach can be justified provided that the correlation between objective video-quality metrics and the plaque-type criterion is sufficiently high.

To evaluate the correlation, we use the method described in [18] to derive Spearman rank order correlation coefficient (SROCC [30]) and Pearson linear correlation coefficient (LCC [30]) between objective VQA algorithms and MOS of the clinical ratings. VQA measurements are fitted beforehand to the clinical ratings provided by the medical experts.

#### E. Material

A total of ten videos, four of the common carotid artery (CCA) and six of the internal carotid artery (ICA) compose our dataset (see Table V). Each video consists of 6.5 s, sufficient for capturing several cardiac cycles. The videos were collected using the standardization protocol described in [22]. This ensures uniform visualization of the plaque morphology. To evaluate the quality of visualization of plaque type and stenosis, we seek to use examples with a large diversity in the sizes of the ROIs. In particular, we are interested in the size of the plaque ROI (see column 2 in Table V) and the size of the wall ROI (see column 3 in Table V). As seen in Table V, we have strong variation for both the plaque ROIs (27–85 MBs) and wall ROIs (132–204 MBs). Overall, we expect larger bandwidth requirements from the larger ROIs.

## IV. RESULTS

We begin with a top-down summary of how we obtained minimum bandwidth requirements. This is followed by a summary of clinical quality assessment and correlation results between objective and subjective evaluations. In the last section, we provide minimum bitrate requirements.

For coarse QP optimization, QP values were varied between 20 and 40 for the atherosclerotic plaque region. Similarly, the sequence frame rate was varied between 5 and 30 frames per second. In addition, the number of inserted RS and the corresponding trade-off between bitrate, transmission time, and error resilience was investigated. The resolution was considered between quarter common intermediate format (QCIF- $176 \times 144$  pixels,  $11 \times 9$  MB) and common intermediate format (CIF- $352 \times 288$  pixels,  $22 \times 18$  MB). This procedure is depicted in Fig. 2(a), while [5]–[7] document preliminary results from these investigations.

The medical experts noted that for a QP of 28, clinical quality is preserved in the compressed video, carrying almost as much clinical information as the original. This led to the fine QP parameter optimization around this value. Thus, a selection of QPs of 28 and lower were found to qualify for clinical practice (see Table III). Fifteen frames per second provided acceptable visualization of clinical motion, while clinical quality deteriorated significantly at less than 10 fps. The CIF resolution was selected, since it provided quality visualization of the plaque morphology, as opposed to issues observed at the QCIF resolution. We note here that CIF resolution video transmission is made possible due to the proposed variable quality slice encoding approach, where achieved bitrate reductions allow the transmission over 3G (and beyond) channels without compromising diagnostic quality. RS utilization was set to one RS for every four coded slices.

Having found an appropriate range of values for the plaque region (being the primary focus point of the clinical evaluation), we then consider slightly higher values (more quantization) for the wall region, and a significantly higher value for the background. A low quantization value for the plaque region allows us to better visualize the echogenic and echolucent areas that are needed for determining the plaque type. A slightly higher quantization is all that is needed for identifying the nearest wall boundary, for visualizing the stenosis. Most of the bandwidth savings come from quantizing the background region. Here, we note that we still need to visualize the background regions to visualize the boundaries and relative motion differences between the plaque and other arterial regions. Furthermore, quantization differences between the plaque and the wall video slices have helped direct clinical attention toward the plaque and its motion relative to the walls (hence stenosis).

For the results from fine QP parameter optimization, we provide a comparative evaluation of: 1) FMO with constant QP video slices; 2) FMO with variable QPs; and 3) FMO with variable QPs with RS for communications in noisy environments. For each method, we had three sets of quantization levels for the video slices.

For comparison, we set QP = 24, 28, and 32 for the plaque video-slice regions for all three cases. Then, for the constant QP case, all video slices are fixed to the plaque QP value. For variable space encoding, we consider 1) low-bandwidth encoding using: QPs = 40/34/32 for the background, wall and ECG, and plaque video slices, respectively; 2) medium-bandwidth encoding with QPs = 38/30/28 (see Fig. 3); and 3) relatively high bandwidth encoding with QPs = 36/26/24. In addition to the

TABLE II  
TOTAL NUMBER OF PROCESSED VIDEOS IN THIS STUDY

|  | Instances  | Cases |
|--|--|-------|
| Method   | FMO, FMO ROI, FMO ROI RS                           | 3     |
| QP <sup>a</sup>                                | 40/34/32, 38/30/38, 36/26/24                       | x3    |
| Packet Loss Rates (PLR)                        | 5%, 8%, 10%, 15%, 20%, 25%, 30%                    | x7    |
| Packet loss simulator                          | Uniform Distribution,<br>averaging 10 runs per PLR | x10   |
| Data Set                                       | 10 videos  | x10   |
| Total number of processed videos in this study |  | 6300  |

<sup>a</sup>FMO scheme uses only 32/32/32, 28/28/28, and 24/24/24.

no packet loss case, at each quantization level, we have seven PLRs: 5%, 8%, 10%, 15%, 20%, 25%, and 30%.

We simulated ten packet loss scenarios for each loss rate and took averages. We thus had three methods  $\times$  3 quantization levels  $\times$  7 loss rates  $\times$  10 simulations per loss rate, for a total of 630 video samples for each of the ten original videos (total = 6300 videos, see Table II).

#### A. Clinical VQA

During the clinical evaluation, the videos were played back on a laptop at their original pixel size dimensions. According to Table I, each diagnostic region received an independent evaluation score. Rating values were between 1 and 5. A rating of 5 was the highest possible. It signified that the clinical capacity of the decoded video was of the same quality as the original (uncompressed) video. A rating of 4 indicated that there was an acceptable loss of minor details. At the lowest scale, a rating of 1 would signify that the decoded video was of unacceptably low quality. As expected, in most cases, higher quality diagnostic ROI encoding resulted in better clinical scores at lower bitrates (compared to the default FMO encoding).

Table III records the MOSs of two medical experts' ratings on the corresponding compressed video instances of the selected QPs range, for the video depicted in Fig. 1(a). Here, Tables III and IV and Fig. 4 depict results obtained for this particular video. We also comment on interobserver variability. The medical experts used in this study each had over ten years experience in assessing ultrasound videos of the carotid artery. In their clinical ratings, we have found that they did not differ by a rating of more than 1 out of a maximum rating of 5. For the criteria listed here, we expect that other clinical experts will give similar ratings. Furthermore, our finding that plaque ROI PSNR values over 35 dB were rated as diagnostically lossless is also in agreement with other studies [8].

We give clinical evaluations for PLR up to 15% for plaque ROI QP of 28 in Table IV. Table IV demonstrates the error resilience of the scheme incorporating RS, even if channel conditions introduce 15% error on the transmitted stream. Furthermore, it depicts the similar behavior as to video degradation of the compared approaches that do not utilize RS. An objective evaluation, shown in Fig. 5, verifies the aforementioned observations for the whole dataset.

Overall, a selection of ROI QPs of 28 and lower were found to qualify for clinical practice. Higher QPs may be selected for urgent clinical practice with respect to bandwidth availability. Having said this, we caution against the use of higher

TABLE III  
CLINICAL EVALUATION MOSS FOR DETERMINING DIAGNOSTICALLY LOSSLESS  
QP. RESULTS ARE FOR THE VIDEO IN FIG. 1(A). CIF RESOLUTION,  
AT 15 FPS, NO ECG LEAD

| FMO                     | QP             | 32/32/32 | 28/28/28 | 24/24/24 |
|-------------------------|----------------|----------|----------|----------|
|                         | BitRate (kbps) | 416      | 788      | 1295     |
| <i>Plaque Detection</i> |                | 5        | 5        | 5        |
| <i>Stenosis</i>         |                | 4.5      | 5        | 5        |
| <i>Plaque Type</i>      |                | 4.5      | 5        | 5        |
| FMO ROI                 | QP             | 40/34/32 | 38/30/28 | 36/26/24 |
|                         | BitRate (kbps) | 191      | 355      | 625      |
| <i>Plaque Detection</i> |                | 5        | 5        | 5        |
| <i>Stenosis</i>         |                | 4.5      | 5        | 5        |
| <i>Plaque Type</i>      |                | 4.5      | 5        | 5        |
| FMO ROI RS              | QP             | 40/34/32 | 38/30/28 | 36/26/24 |
|                         | BitRate (kbps) | 225      | 411      | 700      |
| <i>Plaque Detection</i> |                | 5        | 5        | 5        |
| <i>Stenosis</i>         |                | 4.5      | 5        | 5        |
| <i>Plaque Type</i>      |                | 4.5      | 5        | 5        |

Note: 1: Lowest quality; 5: Highest quality.

Note: QP are given in the order of background/wall ROI/plaque ROI.

TABLE IV  
CLINICAL EVALUATION FOR THE PROPOSED PLAQUE ROI QP OF 28 IN NOISY  
CHANNELS. SEE TABLE III FOR VIDEO DETAILS

|                         | FMO                   | FMO ROI               | FMO ROI RS            |
|-------------------------|-----------------------|-----------------------|-----------------------|
| QP                      | 28/28/28 <sup>a</sup> | 38/30/28 <sup>b</sup> | 38/30/28 <sup>b</sup> |
| BitRate(kbps)           | 788                   | 355                   | 411                   |
| Loss Rates %            | 5/ 8/ 10/ 15          | 5/ 8/ 10/ 15          | 5/ 8/ 10/ 15          |
| <i>Plaque Detection</i> | 4/4.5/4.5/4.5         | 4.5/4.5/4.5/4         | 5/ 5/ 4.5/ 5          |
| <i>Stenosis</i>         | 4/4.5/4.5/4           | 4.5/4.5/4.5/4         | 5/ 5/ 4.5/ 5          |
| <i>Plaque Type</i>      | 3.5/4/3.5/ 4          | 4/ 3.5/ 3.5/ 4        | 4.5/ 4.5/ 4/ 4.5      |

Note: 1: Lowest score, 5: Highest score.

Note: We use FMO, FMO ROI, and FMO ROI RS for constant QP FMO encoding, variable QP FMO encoding, and variable QP FMO with RS, respectively.

<sup>a</sup> 28;background/28;wall ROI/28;plaque ROI.

<sup>b</sup> 38;background/30;wall ROI/28;plaque ROI.

quantization parameter values in ordinary practice. As an example of what can go wrong, we note that in one of the cases [see Fig. 1(c)], an ulcer on the plaque that was still visible for ROI QP of 32 was not visible for ROI QP of 36 (see also [5]). The same observation was true for the video in QCIF resolution.

It's worth noting here an initially surprising finding. For PLR of 15%, the scheme incorporating RS attains higher ratings than when compared to lower PLR of 10%. This detail reveals an important aspect associated with the clinical evaluation of medical videos. Consecutive error-free cardiac cycles may prove sufficient for the physician to reach a diagnosis, even when the objective VQA ratings suggest the opposite. An issue that must be taken into consideration and dictates the need of designing new, diagnostically driven objective VQA algorithms.

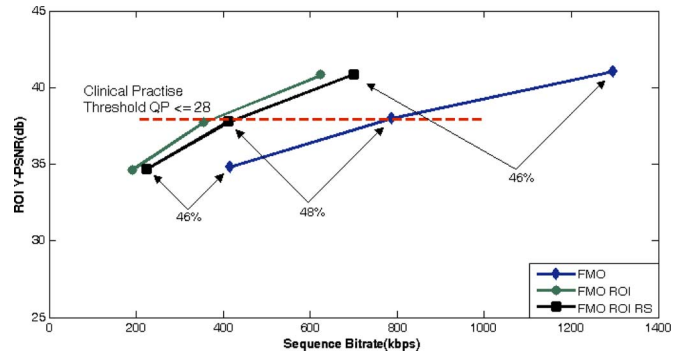


Fig. 4. Rate-distortion curves demonstrating compression efficiency near the diagnostic limit. All three methods are shown for the video of Fig. 1(a). Here, FMO stands for constant QP parameters, FMO ROI denotes the use of variable QP encoding, and FMO ROI RS also uses RSs. The distortion is measured in terms of the PSNR for the plaque ROI. The key point is the significantly reduced sequence bitrate without compromising clinical quality (verified by Table III). Indicatively, for this particular video, FMO ROI RS requires 46%, 48%, and 46% less bitrates than conventional FMO for QPs of 32, 28, and 24, respectively (see text for variable QP parameters). Note that the clinical practice threshold of 35dB or  $QP \leq 28$  is independent of the video.

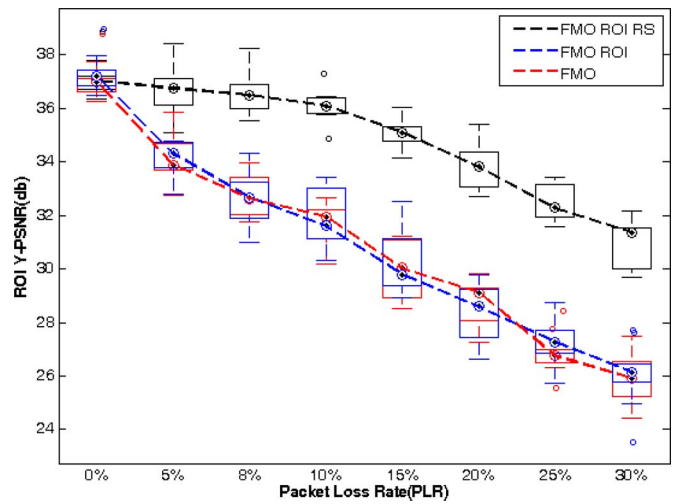


Fig. 5. Quality evaluation for error-prone channels. Here, we evaluate the PSNR versus PLR curve for the plaque ROI (atherosclerotic plaque) QP of 28, by providing box plots for the whole dataset. FMO ROI RS achieves graceful degradation of video quality in the presence of severe loss rates, qualifying for clinical practice even at 15% loss rate. FMO ROI and FMO suffer severe degradation, as evidence by the low PSNR values. Bandwidth requirements reductions are presented in Table V. In each box, the central mark represents the median, the edges represent the 25th and 75th percentiles, and the whiskers extend to the most extreme values. Beyond outliers, extreme points are plotted with hollow circles.

#### B. Objective VQA and Correlation to Clinical Evaluations

For all cases, Table VI summarizes the correlations between the plaque ROI-based VQA algorithms and the MOS from two clinical experts, for clinical ratings for plaque type. SROCC and LCC were deducted by fitting the VQA ratings to a representative sample of 100 video instances. The best results were obtained by ROI-WSNR with an LCC of 0.690 and an SROCC of 0.715. ROI PSNR, SSIM, and VIF algorithms attained scores higher than 0.5.

TABLE V  
DIAGNOSTIC REGIONS OF INTEREST DIMENSIONS AND CORRESPONDING BITRATE SAVINGS (%)

| No.                      | Plaque ROI (pixels, MB) | Wall ROI + opt ECG (MB) | % BitRate Savings for FMO ROI RS vs FMO for ROI QPs 32/28/24 |
|--------------------------|-------------------------|-------------------------|--|
| 1. CCA #1                | 176x64 (44)             | 132+20=152              | 30/38/43   |
| 2. CCA #2                | 144x48 (27)             | 127+20=147              | 45/55/58   |
| 3. CCA #3<br>(Fig. 3)    | 176x48 (33)             | 121+20=141              | 55/60/58   |
| 4. CCA #4                | 160x48 (30)             | 212                     | 34/40/41   |
| 5. ICA #1                | 192x64 (48)             | 194                     | 15/21/27   |
| 6. ICA #2<br>(Fig. 1(b)) | 160x64 (40)             | 202                     | 58/59/55   |
| 7. ICA #3<br>(Fig. 1(c)) | 192x64 (48)             | 150                     | 30/36/37   |
| 8. ICA #4<br>(Fig. 1(a)) | 272x80 (85)             | 135                     | 46/48/46   |
| 9. ICA #5                | 240x64 (60)             | 138                     | 47/51/49   |
| 10. ICA #6 <sup>a</sup>  | 192x80 (60)             | 204+20=224              | 27/31/30   |

<sup>a</sup>Video ICA #6 is an outlier, given that the particular video is a closeup on the atherosclerotic plaque region, and as a result diagnostic ROIs cover almost 72% of the whole video.

Note: %BitRate savings deduced by comparing FMO QPs of 32/32/32, 28/28/28, and 24/24/24 versus FMO ROI RS QPs of 40/34/32, 38/30/28, and 36/26/24.

### C. Minimum Bitrate Requirements

In Table V, bitrate savings of the proposed variable quality FMO with RS scheme when compared to the default FMO scheme are presented. Right column of Table V incorporates the bitrate gains for each of the three quantization level sets for all videos in the dataset. Fig. 6 depicts the required bitrates of all three investigated encoding methods.

To demonstrate some of the typical bandwidth savings, we return to Fig. 4. Here, for the video depicted in Fig. 1(a), we observe bitrate reductions equivalent to 46%, 48%, and 46% for QPs of 40/34/32, 38/30/28, and 36/26/24, respectively, when compared to the default FMO encoding.

The introduction of packet losses produces significant drops in video quality. The drop in video quality more than justifies the overhead of introducing RSs (slightly increased bitrate compared to FMO ROI encoding, see Fig. 6). To see this, we re-examine the example in Fig. 5. At 15% PLR, the use of RSs keeps the clinical video quality at an acceptable level ( $>35$  dB), while all other methods drop below what is acceptable. In fact, there is a 5-dB drop in quality for FMO and FMO ROI that do not use RSs. From Fig. 4, it is clear that both FMO and FMO ROI methods cannot match this performance without a huge increase in bandwidth (which would be off the charts of Fig. 4).

In summary, quantization levels of 40/34/32, 38/30/28, and 36/26/24 match typical available download data rates of 2.5G, 3G, and 3.5G of mobile telecommunication networks, respectively. According to [31], theoretical download data transfer rates extend to 384 kb/s for 2.5G, up to 2 Mb/s for 3G, and 14.4 Mb/s for 3.5G. However, these data rates vary between countries and network operators. Typical data rates are usually between 75–135 kb/s for 2.5G, 220–384 kb/s for 3G, and 400 kb/s–2 Mb/s for 3.5G [2]. Upload data rates are important for real-time m-health systems from remote locations and emergency telemedicine. Latest enhancements in 3.5G, namely,

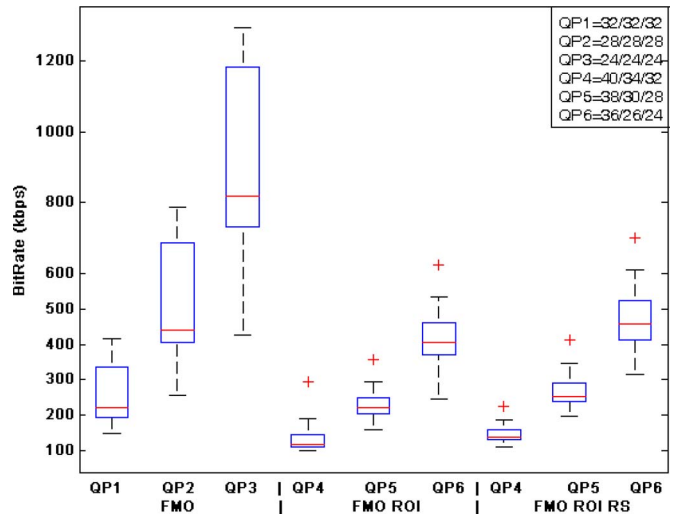


Fig. 6. Box plots for bitrate requirements for the compared schemes for the nine regular videos of the dataset. Here, the last case, in which the video represents a closeup on the plaque is considered an outlier (see Table V for details). We observe that lower quality 40/34/32 (QP4) may be transmitted over 2.5G of mobile communication networks, the recommended case of 38/30/28 (QP5) is well within the typical 3G data rates, while the highest quality of 36/26/24 (QP6) is appropriate for 3.5G networks. In each plot, we display the median, lower, and upper quartiles and confidence interval around the median. Straight lines connect the nearest observations within 1.5 of the interquartile range (IQR) of the lower and upper quartiles. The “+” sign indicates possible outliers with values beyond the ends of the  $1.5 \times \text{IQR}$ .

evolved high-speed packet access, promise 1Mb/s in the uplink (theoretical 40 Mb/s in the downlink and 28 Mb/s in the uplink) [31]. Network operators in Cyprus offer theoretical upload data rates of 384 kb/s and 2 Mb/s for two different 3.5G modems. If the channel data rate input parameter is limited (see Fig. 2), a further quantization of the background may be required for seamless streaming.

### V. DISCUSSION AND CONCLUDING REMARKS

This paper presents a new approach for effective communication of wireless ultrasound video over error-prone channels. Motivated by the need to visualize the plaque boundary, plaque type, and degree of stenosis, we use automated segmentation to identify diagnostic ROIs. These ROIs are mapped to video slices and encoded utilizing FMO type 2. The FMO type 2 concept is modified to support variable quality slice encoding according to the slices’ diagnostic importance. By inserting redundant representations within the transmitted sequence, the encoded video becomes resilient to the presence of extensive PLR. Comprehensive experiments using a dataset composed of ten CIF resolution videos at 15 fps indicate that enhanced diagnostic quality is attained in noisy environments at significantly reduced bitrates. The proposed system setting is summarized in Table VII.

The quality of the decoded videos was evaluated using several objective measures computed over the video slices, and also using clinical ratings. For determining the plaque type, both the (ROI) PSNR and the WSNR gave very good correlations to the MOS provided by two medical experts.

TABLE VI  
COMPARISON OF THE PERFORMANCE OF THE VQA ALGORITHMS FOR PEARSON AND SPEARMAN CORRELATIONS

| ROI/Correlation | PSNR  | SSIM  | VSNR  | VIF   | VIFP  | IFC   | NQM   | WSNR  |
|-----------------|-------|-------|-------|-------|-------|-------|-------|-------|
| LCC             | 0.674 | 0.630 | 0.469 | 0.483 | 0.605 | 0.386 | 0.486 | 0.690 |
| SROCC           | 0.667 | 0.646 | 0.465 | 0.468 | 0.589 | 0.363 | 0.480 | 0.715 |

TABLE VII  
MINIMUM PROPOSED SETTINGS FOR ATHEROSCLEROTIC PLAQUE ULTRASOUND  
VIDEO WIRELESS TRANSMISSION IN NOISY<sup>a</sup> 3G CHANNELS

| Parameter         | Value                                       |
|-------------------|---|
| Encoding Standard | H.264/AVC                                   |
| Profile           | Baseline                                    |
| Error Resilience  | FMO and RS                                  |
| Resolution        | CIF   |
| Frame Rate        | 15 fps ( $\geq$ 10 fps)                     |
| RS                | 1 every 4 slices                            |
| FMO ROI RS QP     | 38/30/28                                    |
| Plaque ROI PSNR   | $\geq$ 35db                                 |
| BitRate           | Typical 3G and beyond<br>rates (see Fig. 6) |

<sup>a</sup>PLRs up to 15%.

Overall, the current study differs from previously published approaches in: 1) the use of efficient encoding based on the current state-of-the-art H.264/AVC standard compared to earlier versions of MPEG-2 [11], [12], MPEG-4 part 2 [12], and motion-JPEG (M-JPEG); 2) the use of error-resilient encoding, such as FMO and RS; 3) efficient variable quality slice encoding based on clinical significance criteria (multiple ROIs) as compared to single-ROI studies in [11]–[13]; 4) extensive simulations for PLR up to 30%; 5) comprehensive subjective and objective VQA, with correlation investigation; and 6) experimentation using a dataset of ten videos with multiple video instances (6300) compared to limited datasets incorporated by corresponding studies in the literature. The findings agree with [8] and [14] that (ROI) PSNR ratings above 35 dB qualify for clinical practice for CIF resolution ultrasound video (QPs of 28 and lower attain higher PSNR ratings than 35 dB, see Fig. 4).

Future work includes extending this study to 4G networks investigating higher quality encodings. A simulation testbed is currently set for this purpose. Further exploitation of objective VQA algorithms for deriving the threshold value, above which diagnostic quality is preserved for each metric, is also planned.

#### ACKNOWLEDGMENT

The authors would like to thank Prof. A. Nikolaides and the Vascular Screening Diagnostic Center, Nicosia, Cyprus for several useful discussions on the diagnostic issues related to the wireless transmission of ultrasound video of the carotid artery, as well as for providing some of the videos of this study. The authors would also like to thank Dr. T. Tyllis for useful discussions and numerous video evaluations.

#### REFERENCES

- [1] R. H. Istepanian, S. Laxminarayan, and C. S. Pattichis, Eds., *M-Health: Emerging Mobile Health Systems*. New York: Springer, 2006, ch. 3.
- [2] E. Kyriacou, M. S. Pattichis, C. S. Pattichis, A. Panayides, and A. Pitsillides, “M-health e-emergency systems: Current status and future directions,” *IEEE Antennas Propag. Mag.*, vol. 49, no. 1, pp. 216–231, Feb. 2007.
- [3] *Advanced Video Coding for Generic Audiovisual Services*, Joint Video Team of ITU-T and ISO/IEC JTC 1, “Draft ITU-T recommendation and final draft international standard of joint video specification (ITU-T Rec. H.264 | ISO/IEC 14496–10 AVC),” Joint Video Team (JVT) of ISO/IEC MPEG and ITU-T VCEG, JVTC050, Mar. 2003.
- [4] M. Hennerici and D. Neuerburg-Heusler, Eds., *Vascular Diagnosis With Ultrasound*. Stuttgart, Germany: Thieme, 1998.
- [5] A. Panayides, M. S. Pattichis, C. S. Pattichis, C. P. Loizou, M. Pantziaris, and A. Pitsillides, “Robust and efficient ultrasound video coding in noisy channels using h.264,” in *Proc. IEEE EMBC’09*, Minnesota, Sep. 2–6, 2009, pp. 5143–5146.
- [6] A. Panayides, M. S. Pattichis, C. S. Pattichis, C. P. Loizou, M. Pantziaris, and A. Pitsillides, “Towards Diagnostically Robust Medical Ultrasound Video Streaming using H.264,” in *Biomedical Engineering*, Carlos Alexandre Barros De Mello, Ed. Vienna, Austria: IN-TECH, 2009, pp. 219–237.
- [7] A. Panayides, M. S. Pattichis, C. S. Pattichis, C. P. Loizou, and M. Pantziaris, “Wireless ultrasound video transmission for stroke risk assessment,” presented at the 5th Int. Workshop Video Process. Quality Metrics Consumer Electron., Scottsdale, AZ, Jan. 13–15, 2010.
- [8] R. S. H. Istepanian, N. Y. Philip, and M.G. Martini, “Medical QoS provision based on reinforcement learning in ultrasound streaming over 3.5g wireless systems,” *IEEE J. Sel. Areas Commun.*, vol. 27, no. 4, pp. 566–574, May 2009.
- [9] S. A. Garawi, R. S. H. Istepanian, and M. A. Abu-Rgheff, “3G wireless communication for mobile robotic tele-ultrasonography systems,” *IEEE Commun. Mag.*, vol. 44, no. 4, pp. 91–96, Apr. 2006.
- [10] M. G. Martini, R. S. H. Istepanian, M. Mazzotti, and N. Philip, “Robust multi-layer control for enhanced wireless tele-medical video streaming,” *IEEE Trans. Mob. Comput.*, vol. 9, no. 1, pp. 5–16, Jan. 2010.
- [11] S. P. Rao, N. S. Jayant, M. E. Stachura, E. Astapova, and A. Pearson-Shaver, “Delivering diagnostic quality video over mobile wireless networks for telemedicine,” *Int. J. Telemed. Appl.*, vol. 2009, pp. 1–9, 2009, Article ID 406753.
- [12] N. Tsapatsoulis, C. Loizou, and C. Pattichis, “Region of interest video coding for low bit-rate transmission of carotid ultrasound videos over 3g wireless networks,” in *Proc. IEEE EMBC’07*, Lyon, France, Aug. 23–26, pp. 3717–3720.
- [13] C. Doukas and I. Maglogiannis, “Adaptive transmission of medical image and video using scalable coding and context-aware wireless medical networks,” *EURASIP J. Wireless Commun. Netw.*, vol. 2008, pp. 1–12, 2008, Article ID 428397.
- [14] P. C. Pedersen, B. W. Dickson, and J. Chakareski, “Telemedicine applications of mobile ultrasound,” presented at the IEEE Int. Workshop on Multimedia Signal Processing, Rio, Brazil, Oct. 5–7, 2009.
- [15] S. Lee, M. S. Pattichis, and A. C. Bovik, “Foveated video quality assessment,” *IEEE Trans. Multimedia*, vol. 4, no. 1, pp. 129–132, Mar. 2002.
- [16] K. Seshadrinathan and A. C. Bovik, “Motion tuned spatio-temporal quality assessment of natural videos,” *IEEE Trans. Image Process.*, vol. 19, no. 2, pp. 335–350, Feb. 2010.
- [17] M. H. Pinson and S. Wolf, “A new standardized method for objectively measuring video quality,” *IEEE Trans. Broadcast.*, vol. 50, no. 3, pp. 312–322, Sep. 2004.
- [18] K. Seshadrinathan, R. Soundararajan, A. C. Bovik, and L. K. Cormack, “Study of subjective and objective quality assessment of video,” *IEEE Trans. Image Process.*, vol. 19, no. 6, pp. 1427–1441, Jun. 2010.
- [19] Z. Wang, A. Bovik, H. Sheikh, and E. Simoncelli, “Image quality assessment: From error measurement to structural similarity,” *IEEE Trans. Image Process.*, vol. 13, no. 4, pp. 600–612, Apr. 2004.
- [20] Metrix\_mux objective video quality assessment software. [Online]. Available: [http://foulard.ece.cornell.edu/gaubatz/metrix\\_mux/](http://foulard.ece.cornell.edu/gaubatz/metrix_mux/) (Retrieved January 2011).

- [21] *Methodology for the subjective assessment of the quality of television pictures*, ITU-R BT.500-12, 2009. [Online]. Available: <http://electronics.ihs.com/collections/itu-r/921b.htm> (Retrieved January 2011).
- [22] C.P. Loizou, C. S. Pattichis, M. Pantziaris, and A. Nicolaides, "An integrated system for the segmentation of atherosclerotic carotid plaque," *IEEE Trans. Inf. Technol. Biomed.*, vol. 11, no. 5, pp. 661–667, Nov. 2007.
- [23] T. Wiegand, G. J. Sullivan, G. Bjøntegaard, and A. Luthra, "Overview of the H.264/AVC video coding standard," *IEEE Trans. Circuits Syst. Video Technol.*, vol. 13, no. 7, pp. 560–576, Jul. 2003.
- [24] S. Wenger, "H.264/AVC over IP," *IEEE Trans. Circuits Syst. Video Technol.*, vol. 13, no. 7, pp. 645–656, Jul. 2003.
- [25] T. Stockhammer, M. H. Hannuksela, and T. Wiegand, "H.264/AVC in wireless environments," *IEEE Trans. Circuits Syst. Video Technol.*, vol. 13, no. 7, pp. 657–673, Jul. 2003.
- [26] S. Wenger and M. Horowitz, "FMO: Flexible macroblock ordering," *JVT-C089*, May 2002. [Online]. Available: [http://wftp3.itiu.int/av-arch/jvt-site/2002\\_05\\_Fairfax/](http://wftp3.itiu.int/av-arch/jvt-site/2002_05_Fairfax/) (Retrieved January 2011).
- [27] P. Lambert, W. De Neve, Y. Dhondt, and R. Van De Walle, "Flexible macroblock ordering in H.264/AVC," *J. Vis. Commun. Image Represent.*, vol. 17, no. 2, pp. 358–375, Apr. 2006.
- [28] H.264/AVC JM 15.1 Reference Software. [Online]. Available: <http://iphone.hhi.de/suehring/tm1/> (Retrieved January 2011).
- [29] S. Park and K. Miller, "Random number generators: good ones are hard to find," *ACM Commun.*, vol. 39, no. 10, pp. 1192–1201, Oct. 1988.
- [30] (2000). Final report from the video quality experts group on the validation of objective quality metrics for video quality assessment. [Online]. Available: [http://www.its.blrdoc.gov/vqeg/projects/frtv\\_phaseI](http://www.its.blrdoc.gov/vqeg/projects/frtv_phaseI)
- [31] GSM World. [Online]. Available: <http://www.gsmworld.com> (Retrieved January 2011).



**A. Panayides** received the B.Sc. degree from the Department of Informatics and Telecommunications, National and Kapodistrian University, Athens, in 2004, and the M.Sc. degree in computing and Internet systems from King's College, London, in 2005. He is currently working toward the Ph.D. degree at the University of Cyprus, Nicosia, Cyprus.

He has authored or coauthored two refereed journal and nine conference papers, and two chapters in books. His research interests include video processing and communications, e-health applications, and mobile telecommunication networks.

Dr. Panayides's Ph.D. study was supported by the Project Real-Time Wireless Transmission of Medical Ultrasound Video IIENEK/ENIΣX/0308/90 funded by the Research Promotion Foundation of Cyprus through the European Regional Development Fund (ERDF).



**M. S. Pattichis** (M'99–SM'06) received the B.Sc. (highest honors and special honors) degree in computer sciences and the B.A. (highest honors) degree in mathematics, both in 1991, the M.S. degree in electrical engineering, in 1993, and the Ph.D. in computer engineering, in 1998, all from the University of Texas at Austin, Austin.

He is currently an Associate Professor in the Department of Electrical and Computer Engineering, University of New Mexico (UNM), Albuquerque. His research interests include digital image, and video processing and communications, dynamically reconfigurable computer architectures, and biomedical and space image-processing applications.

Dr. Pattichis is an Associate Editor of the IEEE TRANSACTIONS ON IMAGE PROCESSING and was an Associate Editor for the IEEE TRANSACTIONS ON INDUSTRIAL INFORMATICS, and a Guest Associate Editor for the IEEE TRANSACTIONS ON INFORMATION TECHNOLOGY IN BIOMEDICINE. He was the General Chair of the 2008 IEEE Southwest Symposium on image analysis and interpretation. He was a recipient of the 2004 Electrical and Computer Engineering Distinguished Teaching Award and the 2006 School of Engineering Harrison Faculty Recognition Award at UNM.



**Constantinos S. Pattichis** (S'88–M'88–SM'99) was born in Cyprus, on January 30, 1959. He received the Diploma of Technician Engineer degree in electrical Engineering, from the Higher Technical Institute, Cyprus, in 1979, the B.Sc. degree in electrical engineering from the University of New Brunswick, Canada, in 1983, the M.Sc. degree in biomedical engineering from the University of Texas, Austin, in 1984, the M.Sc. degree in neurology from the University of Newcastle Upon Tyne, Tyne, U.K., in 1991, and the Ph.D. degree in electronic engineering from the University of London, London, U.K., in 1992.

He is currently a Professor in the Department of Computer Science, University of Cyprus, Nicosia, Cyprus. He has been involved in numerous projects funded by the EU, the National Research Foundation of Cyprus, the INTERREG, and other bodies, like the MEDUCATOR, LONG LASTING MEMORIES, INTRAMEDNET, INTERMED, FUTURE HEALTH, AMBULANCE, EMERGENCY, ACSRS, TELEGYN, HEALTHNET, IASIS, and IPPOKRATIS, with a total funding managed more than six million Euros. He has published 64 refereed journal and 160 conference papers, and 24 chapters in books. He is also a coauthor of the monograph *Despeckle Filtering Algorithms and Software for Ultrasound Imaging* (Morgan & Claypool Publishers, 2008). He is a Coeditor of the books *M-Health: Emerging Mobile Health Systems* (New York: Springer, 2006) and *Ultrasound and Carotid Bifurcation Atherosclerosis* (New York: Springer, 2011). He was a Guest Coeditor of the special issues on Emerging health telematics applications in Europe, emerging technologies in biomedicine, Computational intelligence in medical systems, and Citizen centered e-health systems in a global health-care environment of the IEEE TRANSACTIONS ON INFORMATION TECHNOLOGY IN BIOMEDICINE. During 2005–2007, he was an Associate Editor for the IEEE TRANSACTIONS ON NEURAL NETWORKS, and he has been an Associate Editor of the IEEE TRANSACTIONS ON INFORMATION TECHNOLOGY IN BIOMEDICINE, since 2000. His research interests include e-health, medical imaging, biosignal analysis, and intelligent systems.

He was the General Cochairman of the Medical and Biological Engineering and Computing Conference (MEDICON'98), the IEEE Region 8 Mediterranean Conference on Information Technology and Electrotechnology (MELECON'2000), and the IEEE Information Technology in Biomedicine (ITAB09), and Program Cochair of ITAB06, and the 4th International Symposium on Communications, Control and Signal Processing (ISCCSP 2010). He is on the Editorial Board of the *Journal of Biomedical Signal Processing and Control*. He was the Chairperson of the Cyprus Association of Medical Physics and Biomedical Engineering during 1996–1998, and the IEEE Cyprus Section during 1998–2000.



**C. P. Loizou** (M'05) received the B.Sc. degree in electrical engineering and the Dipl.-Ing. (M.Sc.) degree in computer science and telecommunications from the University of Kaiserslautern, Kaiserslautern, Germany, in 1986 and 1990, respectively, and the Ph.D. degree in ultrasound image analysis of the carotid artery from the Department of Computer Science, Kingston University, London, U.K., in 2005.

From 1996 to 2000, he was a Lecturer in the Department of Computer Science, Higher Technical Institute, Nicosia, Cyprus. Since 2000, he has been an Assistant Professor in the Department of Computer Science, School of Sciences and Engineering, Intercollege, Cyprus. He was a Supervisor for a number of Ph.D. and B.Sc. students in computer image analysis and telemedicine. He is also an Associate Researcher at the Institute of Neurology and Genetics, Nicosia, Cyprus. He is the author or coauthor of the book *Despeckle Filtering Algorithms and Software for Ultrasound Imaging*, 14 chapters in books, 14 referred journals, and 55 conference papers in image and video analysis. His current research interests include medical imaging and processing, motion and video analysis, signal and image processing, pattern recognition, biosignal analysis, in ultrasound, magnetic resonance, and optical coherence tomography imaging and computer applications in medicine.

Dr. Loizou is a Senior Member of the Institution of Electrical Engineers.



**M. Pantziaris** received the M.D. degree in neurology from the Aristotelion University, Thessaloniki, Greece, in 1995.

During 1995, he was trained in carotid duplex-Doppler ultrasonography at St. Mary's Hospital, London. During 1999, he was a Visiting Doctor in acute stroke treatment at Massachusetts General Hospital, Harvard University, Boston. He is currently a Senior Neurologist in the Neurological Department, Cyprus Institute of Neurology and Genetics, Nicosia, Cyprus, and is also the Head of the Neurovascular Department. He has considerable experience in carotid-transcranial ultrasound. He has participated in many research projects, and has several publications to his name. He is also the Head of the Multiple Sclerosis (MS) Clinic, where he is involved in the research on the etiology and therapy of MS.



**Andreas Pitsillides** (M'90–SM'05) received the B.Sc. degree (Hons.) in electrical engineering from the University of Manchester Institute of Science and Technology (UMIST), Manchester, U.K., and the Ph.D. degree in broadband networks from the Swinburne University of Technology, Melbourne, Australia, in 1980 and 1993, respectively.

Currently he is a Professor in the Department of Computer Science, University of Cyprus, Nicosia, Cyprus, where he is also the Head of the Networks Research Laboratory. He has published more than

210 research papers and book chapters, and has participated in over 30 European Commission and locally funded research projects with over 4.5 million Euro as Principal or Co-Principal Investigator. He is a Coeditor of the book *Modeling and Control of Complex Systems* (CRC Press, 2007). He has presented keynotes and invited lectures at major research organizations and universities, and also has given short courses at international conferences and short courses to industry. His research interests include fixed and wireless networks, flow and congestion control, resource allocation and radio resource management, and Internet technologies and their application in mobile e-services, and the Web of Things. He has a particular interest in adapting tools from various fields of applied mathematics, such as adaptive nonlinear control theory, computational intelligence, and nature-inspired techniques, to solve problems in communication networks.

Prof. Andreas Pitsillides was on the Executive Committees of major conferences, e.g., the International Conference on Telecommunications (ICT) 2011 and 1998, the IEEE International Conference on Computer Communications (INFOCOM) 2001, 2002, and 2003, Symposium on Modeling and Optimization in Mobile, Ad Hoc, and Wireless Networks (WiOpt) 2007, the International Conference on Intelligent Systems and Computing: Theory and Applications (ISYC) 2006, and the Workshop on Modeling and Control of Complex Systems (MCCS) 2005. He is a member of the International Federation of Automatic Control (IFAC) Technical Committee TC 1.5 on Networked Systems and TC 7.3 on Transportation Systems, and the International Federation of Information Processing (IFIP) working group WG 6.3: Performance of Communications Systems. He is also a member of the Editorial Board of the *Computer Networks* (COMNET) and the *International Journal of Handheld Computing Research* (IJHCR).